THE EXCITED ATOMIC HYDROGEN LINES 126α AND 127α IN HII REGIONS

By R. X. McGee* and F. F. Gardner*

Summary

Forty radio sources have been observed for the presence of the hydrogen recombination lines 126α at 3248·708 MHz and 127α at 3172·864 MHz with a 6′ arc aerial beam and a receiver with 48 channels of 37 kHz bandwidth each. Detections were made in 34 sources, all of which were either HII regions or optically unidentified thermal sources.

The mean ratio of line intensity to thermal continuum intensity was 3·4% (±1·3% s.d.); the mean halfwidth of the lines was 340 kHz (±50 kHz s.d.), which is equivalent to 31·5 km/sec in radial velocity.

It is suggested that many of the profiles are complex and contain two or more major components that represent large-scale motions in the HII regions. The Orion and Omega nebulae are shown to have this type of profile and are discussed in some detail.

I. INTRODUCTION

The detection of the lines of atomic hydrogen in interstellar space by observing transitions between energy levels of high principal quantum numbers had not been seriously considered (e.g. Wild 1952) until Kardashev (1959), using the theory developed by Menzel and Pekeris (1935), showed that in HII nebulae the expected intensities and line widths in the decimetre wavelength band made investigation worth while.

Dravskikh and Dravskikh (1964) reported that the excited H line $n = 105$ to 104 had been observed in the Orion and Omega nebulae, while Sorochenko and Borodzich (1964) reported similar observations for 90α. Since then the n α-lines (i.e. emission lines from principal quantum numbers $n+1$ to n) for $n = 94, 109, 126, 156, 158, 166,$ and 253 have been investigated in a number of HII nebulae.

The physical quantities most conveniently measured are the ratio of the intensities of the emission line and the thermal continuum background and the line halfwidth. Several authors (Höglund and Mezger 1965; Lilley *et al.* 1966; Palmer and Zuckerman 1966; Penfield, Palmer, and Zuckerman 1967) have used the product of these two quantities to compute the electron temperature of HII nebulae. The values thus obtained have been less than 6000°K rather than near the 10000°K derived from many optical measurements. Comments on such results have been made by Goldberg (1966), Weedman (1966), and the present authors (Gardner and McGee 1967; McGee and Gardner 1967); further explanation is offered here in discussing the results of the present survey. It is suggested that in a number of cases the observed profiles contain more than one component of systematic motion and may not be suitably represented by single Gaussian curves.

* Division of Radiophysics, CSIRO, Box 76, P.O. Epping, N.S.W. 2121.

The 126α and 127α recombination H lines at frequencies 3248·708 and 3172·864 MHz respectively have been sought in 40 objects. They have been detected in 34, all of which are either recognized as HII nebulae or are optically unidentified thermal radio sources.

II. Theoretical Relationships between the Quantities Measured

The total energy emitted per unit volume per second by an assembly containing N_n atoms per unit volume in quantum state n is (e.g. Menzel and Pekeris 1935)

$$P_{\nu,\text{line}} = N_n A_{nn'} h\nu$$

$$= \int_0^\infty I(\nu)\, d\nu = I_{\text{peak}} \Delta w, \tag{1}$$

where I_{peak} and Δw refer to the peak intensity and the equivalent width in terms of the peak intensity, and from Menzel (1937)

$$N_n = \frac{b_n N_i N_e h^3}{(2\pi m k T_e)^{3/2}} \frac{g_n}{2} \exp(hRZ^2/n^2kT).$$

In the present case (for hydrogen atoms and $n = 126$) only the first term of the expansion of the exponential is significant (the second term is less by a factor of 10^{-14}), and we write

$$N_n = \frac{b_n N_i N_e h^3}{(2\pi m k T_e)^{3/2}} \frac{g_n}{2}.$$

$A_{nn'}$, the Einstein probability coefficient for spontaneous transition from state n to n', is given by

$$A_{nn'} = \frac{g_{n'}}{g_n} \frac{8\pi^2 e^2 \nu^2}{mc^3} f_{nn'},$$

where g_n and $g_{n'}$ are the statistical weights for the n and n' levels and $f_{nn'}$ is the number of dispersion electrons per atom, or the oscillator strength; $f_{nn'} = un$. Kardashev (1959) gives $u = 0·18$, but Sorochenko (1965) gives a value of $0·15$.*

For a discrete state of hydrogen $g_n = 2n^2$. b_n is a numerical factor ($0 < b_n \leqslant 1$) that is used to include departures from thermodynamic equilibrium; at local thermodynamic equilibrium $b_n = 1$ (see, for example, Seaton 1964).

The continuum temperature of the HII nebula is measured simultaneously with the line temperature. Using the expression derived for the emission coefficient (e.g. Oster 1961), we can write for the power per unit volume

$$P_{\nu,\text{continuum}} = \frac{32 N_e N_i Z^2 e^6 (2\pi m)^{\frac{1}{2}}}{3 m^2 c^3 (kT_e)^{\frac{1}{2}}} \ln \left(\frac{(2k)^{3/2}}{\pi e^2 m^{\frac{1}{2}} \gamma^{5/2}} \frac{T_e^{3/2}}{\nu} \right), \tag{2}$$

where, in equations (1) and (2), N_e and N_i are the numbers of electrons and ions per unit volume, Z is the atomic number, e the electronic charge, m the electron mass,

---

* *Note added in proof.* After evaluating oscillator strengths on a computer Dr. P. Palmer (personal communication) finds $u = 0·19$ is more accurate.

c the velocity of light, k Boltzmann's constant, h Planck's constant, T_e the kinetic temperature of the electrons, $\gamma = 1\cdot 7807$ (derived from Euler's constant), and ν the line frequency. If T_1 is the observed peak value of the line temperature, which is measured above T_c, the thermal continuum temperature, equations (1) and (2) may now be combined to give $(T_1/T_c)\Delta\nu$ in terms of atomic hydrogen constants, kinetic temperature, and frequency as

$$\left(\frac{T_1}{T_c}\right)\Delta\nu = \left(\frac{4\ln 2}{\pi}\right)^{\frac{1}{2}} \frac{3h^4 b_n\,unn'^2\nu^3}{16mke^4 T_e\,\ln\left[\{(2k)^{3/2}/\pi m^{\frac{1}{2}}e^2\gamma^{5/2}\}\{T_e^{3/2}/\nu\}\right]}. \tag{3}$$

The first term on the right-hand side of this equation is the correction from Δw to a half-power width for a Gaussian line shape ($\Delta\nu$). It is assumed in (3) that the line shape is a single Gaussian and that the optical depth for both radiations is low.
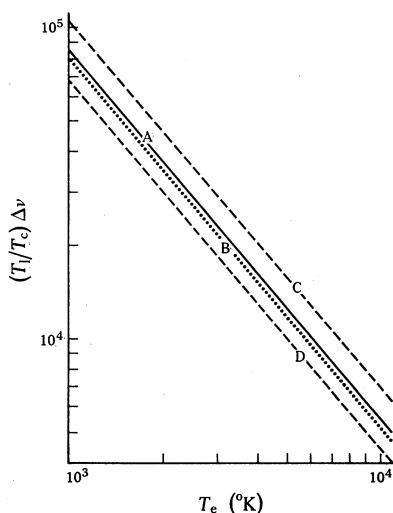

Fig. 1.—Relation between $(T_1/T_c)\Delta\nu$ and the kinetic temperature T_e of electrons in the nebulae for (A) $n = 126$ at local thermodynamic equilibrium, $b_n = 1$, $u = 0\cdot 15$; and (B) $n = 127$, $b_n = 1$, $u = 0\cdot 15$. The dashed lines C ($b_n = 1$, $u = 0\cdot 19$) and D ($b_n = 0\cdot 8$, $u = 0\cdot 15$) show the effects of changes in u up to $0\cdot 19$ and departure from local thermodynamic equilibrium to $b_n = 0\cdot 8$.

In Figure 1 $(T_1/T_c)\Delta\nu$ is plotted against T_e between 1000 and 11000°K for $n = 126$, $b_n = 1$, and $u = 0\cdot 15$ (line A). The dashed lines indicate limits by values $b_n = 0\cdot 8$, $u = 0\cdot 15$ (line D), and $b_n = 1$, $u = 0\cdot 19$ (line C). The relation for $n = 127$, $b_n = 1$, $u = 0\cdot 15$ is given by the dotted line (B). The values used in the calculations were taken from the report on fundamental constants by Cohen and Du Mond (1965).

Although not attempted here, the calculations combined with observational results may be carried further, if information on electron density is available and certain assumptions are made, to produce the r.m.s. velocity of internal turbulence in an HII region (see, for example, Mezger and Höglund 1967).

III. METHODS AND OBSERVATIONS

The observations were made with the 210 ft radio telescope of the Australian National Radio Astronomy Observatory at Goobang Valley near Parkes, N.S.W. The aerial beamwidth at 3250 MHz was measured as 6′ arc. The receiver had an overall system noise temperature of 300°K approximately on the cold sky. The

crystal mixer input accepted both sidebands with the first intermediate frequency at $30 \cdot 43$ MHz. For observation of the line a second conversion was made to the main amplifier at $6 \cdot 74$ MHz, where the output was split into 48 channels of filters and detectors. The filter widths were 37 kHz spaced at intervals of 33 kHz. The continuum or total-power channel of width 3 MHz was detected at the 30 MHz amplifier to give T_c. A description of the back end of the receiver is given by McGee and Murray (1963). The local oscillators, derived from tunable oscillators near 6 MHz in frequency, were switched between the "signal" band and a "reference" band $2 \cdot 16$ MHz away, which was well outside the line frequency band. Intensity calibrations were made from time to time using a noise lamp modulated in synchronism with the switching frequency and introduced at the receiver input by means of a directional coupler. The frequencies were continually monitored.

In making an observation four profiles, each requiring a time of 2 min, were recorded at the position of the maximum of the continuum intensity and four at a neighbouring reference position, usually at the same declination but of such right ascension that the zenith angle of the telescope was the same at each position. The effects of changes in baseline with zenith angle were largely eliminated in this way. The procedure was repeated until a sufficiently good signal-to-noise ratio was achieved for the observation. The r.m.s. fluctuations per channel were calculated from several series of test observations. Average values for the 48 channels for single profiles were $\pm 0 \cdot 63$ degK at $3248 \cdot 7$ MHz and $\pm 0 \cdot 42$ degK at $3172 \cdot 9$ MHz. These values are in satisfactory agreement with the measured system noise temperature mentioned above.

The observations of the 126α line at $3248 \cdot 7$ MHz were made in the upper side-band and the equivalent radial velocity (derived from the frequency difference) was such that it was increasing in value from channel 1 to channel 48. The observations of the 127α line at $3172 \cdot 9$ MHz were made in the lower sideband and hence the radial velocity was decreasing in value from channels 1 to 48. When both lines were observed in a source the entirely different receiver conditions served as a means of confirming or rejecting features of doubtful nature. At the 126α line the conversion of frequency to radial velocity is such that 1 km/sec $= -10 \cdot 8365$ kHz; at the 127α line, 1 km/sec $= -10 \cdot 5835$ kHz.

The original data were corrected for gain and baseline differences in the various channels, averaged, and plotted in the CDC 3200 computer of the Division of Computer Research, CSIRO.

The HII nebulae (and other thermal sources) investigated in the survey include most of the more intense southern Milky Way radio sources, all of which have been previously observed for the presence of OH emission or absorption (McGee, Gardner, and Robinson 1967). Some nonthermal sources were used as controls. Several northern sources were observed so that comparisons of radial velocities and spectra of T_1/T_c and $\Delta \nu$ against frequency could be studied.

IV. RESULTS

Forty sources were observed for at least one of the 126α or 127α lines; some were checked for angular extensions and possible changes in velocity in the line-emitting regions by making observations at half-beamwidth intervals around them.

The astronomical and physical data are listed in Table 1. Columns 1–5 contain the source name, the right ascension and declination (epoch 1950·0), and the galactic coordinates l^{II} and b^{II}. Column 6 shows which lines were observed.

The observational data begin with the continuum aerial temperature T_c in column 7 of Table 1. The maximum intensity of the continuum radiation was located for each source before line observations were made. This followed the same procedure as for the absorption lines in the OH survey (McGee, Gardner, and Robinson 1967). Owing to the improved angular resolution, the confusion effects of the blending of sources with background radiation or other sources were reduced. As a result, all the positions in column 7 differ by a few minutes of arc from the 1660 MHz (OH line) positions. Additional sources (marked "II" and "III" in column 1) were discovered near η Carinae, 1308—62, 1617—50, and NGC 6357.

Columns 8, 9, 12, and 13 of Table 1 contain the observed line data: the radial velocity (km/sec) at the profile peak intensity referred to the local standard of rest (l.s.r.); the aerial temperature of the line T_l (°K); and the line halfwidth $\Delta\nu$ (kHz and km/sec) measured between points of half the maximum intensity. The equivalent r.m.s. noise (degK) is given in column 10. It varies according to the number of profiles included in each observation—the overall average is $\pm 0\cdot 26$ degK. An additional uncertainty not included here is caused by the slight alterations in baseline from one set of profiles to another taken at a different time but combined to complete the "observation". Two approaches have been made in deciding the shape of the observed profile. One author has fitted the best possible Gaussian curve to each set of points. The other has fitted a curve to the points as closely as possible, established a baseline from the trends on either side of the line, and made the above measurements. Good agreement was found for the radial velocities and line temperatures, but the Gaussian curves tended to be wider by an average of about $3\cdot 5$ km/sec. The values given are compromises obtained by combination and suitable weighting of both sets of measurements. However, in some important cases the latter method revealed more than one profile peak. This aspect will be discussed in the next section.

The ratio of the temperature of the line to the thermal continuum and the product of this ratio with the halfwidth are given in columns 11 and 14 of Table 1.

It will be noticed that, although two lines (126α and 127α) have been observed, in many cases the results have been averaged. The effective signal-to-noise ratio is not good enough to give separate sets of information from the neighbouring lines.

The remaining columns 15 and 16 of Table 1 contain the OH-line radial velocities (rounded off) and references to remarks given as footnotes to the table.

(a) Comments on Table 1

(i) Surrounding Points

In the five sources Orion Nebula, RCW 38, η Carinae, NGC 6334, and Omega Nebula we have made observations at surrounding points (usually at approximately half-beamwidth spacing) to determine any marked spread or changes in the area of recombination line emission. At the present sensitivity and angular resolution only

TABLE 1

POSITIONS OF SOURCES AND PHYSICAL CHARACTERISTICS OF EXCITED HYDROGEN

(1)	(2)	(3)	(4)	(5)	(6)	(7)	(8)	(9)	(10)	(11)	(12)	(13)	(14)	(15)	(16)
Source	Position (1950·0) R.A. (h m s)	Dec. (° ′)	Galactic Coordinates l^{II} (°)	b^{II} (°)	α Line Obs.*	T_c (°K)	R.V. at Line Peak (km/sec)	T_1 (°K)	R.M.S. Noise (±degK)	T_1/T_c (%)	Halfwidth $\Delta\nu$ (kHz)	$\Delta\nu$ (km/sec)	$\frac{T_1}{T_c}\Delta\nu$ (kHz)	R.V. of OH Lines (km/sec)	Remarks†
Crab Nebula	05 31 30	+21 59·1	184·5	−5·8	6	364	—	—	0·4	—	—				
	05 31 46	+21 59·1	184·6	−5·7	6, 7	178	—	—	0·3	—	—				
Orion Nebula	05 32 50	−05 25·8	209·0	−19·4	6, 7	183	−7‡	4·4	0·1	2·4	406	38	9·74	+8, +3, +21	1
Orion Δα−3′	05 32 37	−05 25·7	209·0	−19·4	6, 7	100	−7‡	2·1	0·3	2·1	342	32	7·17		
Orion Δα+3′	05 33 02	−05 25·7	209·0	−19·3	6, 7	109	−5‡	2·8	0·3	2·6	332	31	8·63		
Orion Δδ−3′	05 32 50	−05 28·7	209·0	−19·4	6	110	−7‡	2·7	0·3	2·5	410	38	10·25		
Orion Δδ+3′	05 32 50	−05 22·3	209·0	−19·4	6	105	−1‡	2·5	0·3	2·4	410	38	9·85		
30 Doradus	05 39 05	−69 06·9	279·4	−31·7	6	13	—	—	0·2	—	—				
NGC 2024	05 39 10	−01 56·0	206·5	−16·4	6, 7	30	+4	1·0	0·2	3·3	225	21	7·43		
IC 443	06 14 48	+22 48·4	188·9	+3·2	6	3	—	—	0·3	—	—				
RCW 38	08 57 20	−47 19·5	267·9	−1·1	6, 7	97	+1	1·9	0·2	2·0	320	30	6·40	+1, +3	
RCW 38 Δα−3′	08 57 02	−47 19·5	267·9	−1·1	6	39	+11	0·6	0·4	1·6	380	35	6·08		
RCW 38 Δα+3′	08 57 38	−47 19·5	268·0	−1·0	6	75	+2	1·4	0·4	1·9	270	25	5·12		2
RCW 38 Δδ−3′	08 57 20	−47 22·5	268·0	−1·1	6	48	−3	1·0	0·4	2·1	270	25	5·66		
RCW 38 Δδ+3′	08 57 20	−47 16·5	267·9	−1·0	6	62	(−1)	(1·3)	0·4	(2·1)	(380)	(35)	(7·98)		
RCW 36	08 57 34	−43 34·3	265·1	+1·4	7	12	−3	0·8	0·2	6·7	380	36	25·5	+11, +27	
RCW 46	10 04 54	−56 58·5	282·0	−1·2	7	14	+19	0·7	0·2	5·0	233	22	11·65	−8, 0, +3, +7	
RCW 49	10 22 22	−57 31·7	284·3	−0·3	6, 7	62	−2	1·7	0·2	2·8	290	27	8·12	−20	
η Carinae I	10 41 47	−59 19·9	287·4	−0·6	6, 7	37	−20	1·3	0·1	3·4	396	37	13·47	−21	
η Car Δα−3′	10 41 23	−59 19·9	287·6	−0·7	6	31	−16	1·1	0·4	3·5	325	30	11·40		
η Car Δα+3′	10 42 11	−59 19·9	287·5	−0·6	6	28	—	—	0·4	—	—				
η Car Δδ−3′	10 41 48	−59 22·9	287·8	−0·7	6	30	—	—	0·4	—	—				
η Car Δδ+3′	10 41 47	−59 16·9	287·9	−0·6	6	30	−20	1·0	0·4	3·3	347	32	11·46		
η Carinae II	10 42 52	−59 22·6	287·9	−0·6	6	34	−40	1·1	0·2	3·2	(304)	(28)	9·72		
							−1	0·8		2·4	(270)	(25)	6·48		
1109−61	11 09 49	−61 02·7	291·3	−0·7	6	52	−23	1·0	0·3	2·0	433	40	8·66		
							+30	0·6	0·3	1·2	304	28	3·64		
RCW 57	11 12 58	−60 59·2	291·6	−0·5	6	67	+10	1·5	0·2	2·2	422	39	9·30	−8	3
1207−62	12 07 18	−62 33·6	298·2	−0·3	7	17	+11	0·5	0·2	3·2	264	25	8·45	−52, +4	
1308−62I	13 09 09	−62 18·9	305·3	+0·2	6, 7	22	−49	0·5	0·2	2·5	(278)	(26)	6·95	−44, −39	
							−30	0·8	0·2	3·6	(278)	(26)	10·00	−36	
1308−62II	13 08 09	−62 29·5	305·2	0·0	7	14	−50	1·0	0·2	7·1	(339)	(32)	24·10		
							−13	0·6	0·2	4·3	(318)	(30)	13·68		
1386A	13 43 37	−60 08·1	309·8	+1·7	7	11			0·2	—	—				

Source	R.A.	Dec.	l	b	*										†
1404−61	14 04 07	−61 13·6	311·9	+0·1	7	4·5	—	—	0·2	—	—			−8	
1441−59	14 41 26	−59 37·8	316·8	−0·1	7	17	—	—	0·2	—	—			−37, −26	4
1442−59	14 42 04	−59 11·7	317·0	+0·3	7	4·5	—	—	0·2	—	—			−19	
1540−53	15 40 55	−53 58·5	326·6	+0·6	7	16·5	(−45)	(0·5)	0·2	(3·0)	318	30	9·55	−31, −15	5
1549−54	15 49 07	−54 26·9	327·3	−0·5	7	26	−62	1·1	0·2	4·3	(318)	(30)	13·70	−94, −54	
							−19	0·9	0·2	3·5	(318)	(30)	11·14	−51, −43, −26	
1608−51	16 08 14	−51 19·5	331·5	−0·1	6,7	18	−91	0·7	0·2	4·0	310	29	12·40	−101, −97, −90	
1617−50I	16 17 01	−50 31·8	333·1	−0·4	6,7	20	−48	1·2	0·2	6·0	328	31	19·70	−59, −45	
1617−50II	16 17 40	−50 19·6	333·3	−0·4	7	20	−59	1·7	0·2	3·0	(381)	(36)	11·43		
							−11	1·5	0·2	2·5	(286)	(27)	7·15		5
1618−49	16 18 22	−49 59·3	333·6	−0·2	6,7	38·5	−57	1·1	0·2	2·8	(354)	(33)	9·90	−115, −73	6
							−28	1·1	0·2	2·8	(440)	(41)	12·33	−55, −31, −22, +8	
1630−47	16 30 46	−47 29·7	336·8	+0·1	7	14·5	−71	0·5	0·2	3·6	275	26	9·88	−120, −53	
1637−46	16 37 03	−46 17·4	338·4	+0·1	7	13·5	−38	0·6	0·2	4·2	381	36	16·00	−92, −24	
1716−38	17 16 35	−38 55·2	348·7	−1·0	7	21	−6	0·4	0·2	2·1	423	40	8·88	+31	
							+69	0·7	0·2	3·3	413	39	13·64		
NGC 6334	17 17 09	−35 47·1	351·3	+0·7	6,7	40	−4	2·2	0·2	5·4	374	35	20·25	−5, +6	
Source A	17 17 32	−35 43·8	351·4	+0·6	6	20	−4	1·0	0·3	5·0	390	36	19·51	−12, −8, −11	
Source B	17 16 34	−35 55·8	351·1	+0·7	6	11	—	—	—	—	—			−9, −6, −13	
NGC 6357I	17 21 24	−34 08·6	353·2	+0·9	6	45	−5	1·3	0·3	2·8	368	34	10·30		
NGC 6357II	17 22 17	−34 20·0	353·3	+0·6	6	38	−1	1·1	0·2	2·9	324	30	9·39	−11, −6, +1, +5	
NGC 6357III	17 22 42	−34 15·6	353·2	+0·6	6	23·5	−1	1·6	0·4	6·8	260	24	17·70		
SGR A	17 42 28	−28 59·5	359·9	−0·0	6,7	129	—	—	0·3	—	—				
SGR B₂	17 44 09	−28 23·6	0·6	−0·0	6,7	26	—	—	0·2	—	—				7
M 8	18 00 35	−24 23·7	005·9	−1·2	6	21·5	−4	0·6	0·3	2·8	347	32	9·71		
Omega Nebula (M 17)	18 17 34	−16 12·7	015·0	−0·7	6	183	+9	4·5	0·1	2·5				+20	8
							+19	6·0	0·1	3·3	390	36	10·40		
							+32	4·1	0·1	2·2					
M 17 $\Delta\alpha-4'$	18 17 20	−16 12·1	015·0	−0·6	6	94	+18‡	2·9	0·4	3·1	347	32	10·77		
M 17 $\Delta\alpha+4'$	18 17 52	−16 12·1	015·0	−0·7	6	90	+17‡	2·4	0·4	3·7	390	36	14·45		
M 17 $\Delta\delta-4'$	18 17 37	−16 16·1	015·0	−0·7	6	107	+19‡	3·6	0·4	3·4	369	34	12·56		
M 17 $\Delta\delta+4'$	18 17 38	−16 08·1	015·1	−0·7	6	100	+18‡	3·6	0·4	3·6	390	36	14·05		
W 43	18 44 59	−02 00·9	030·7	−0·0	7	38·5	+89	0·8	0·2	2·2	286	27	6·29		
W 49	19 07 52	+09 01·8	043·2	−0·4	6	30	+7	1·9	0·3	6·4	282	26	18·07	+6, +13, +16, +18, +22	
W 51	19 21 26	+14 25·0	049·5	−0·4	6	50	+55	2·1	0·3	4·2	400	37	16·80		

* 6 = 126α, 7 = 127α.

† Relevant remarks are: 1. Peaks occur at −10, +1, and +18 for the median value of −7 km/sec (column 8). 2. +6·5 mean. 3. There was a bad baseline for measurements. 4. There is a possible line at −36 km/sec. 5. Results are doubtful. 6. There is an intermediate peak at −46 km/sec, $T_1/T_c = 3·2\%$. 7. See Section IV (a) (iii). 8. The median value is +17 km/sec.

‡ Median values.

the median radial velocities have been considered. Some remarks on the five sources follow.

Orion Nebula. The radial velocity is more positive at the northern point (−1 km/sec) with a similar tendency at the eastern point (−5 km/sec) than at the central position (−7 km/sec, median).

RCW 38. The observations have a rather poor signal-to-noise ratio. The profile at the western point has a median value of +11 km/sec but a peak occurs at +2 km/sec. The central-point median velocity is +1 km/sec.

η Carinae. Any line signal at the eastern and southern points is lost in noise. The northern and western observations indicate that the source of excited H line may be displaced in their directions.

NGC 6334. The additional observations were made at the positions of OH emission—sources A and B. The same velocity as at the continuum maximum was measured at A; no line was detected at B.

Omega Nebula. There is an indication that the radial velocity is less positive at the northern and eastern points (+16 km/sec) than at the southern and western points (+19 and +18 km/sec respectively). The central point is at +17 km/sec median velocity.

(ii) *Companion Sources*

Excited H lines were observed at more than one continuum peak in five of the thermal sources. They are designated: η Carinae I and II, RCW 57 and 1109−61, 1308−62 I and II, 1617−50 I and II, and NGC 6357 I, II, and III.

(iii) *Negative Results*

Ten cases were found where no line signal was detected above the noise. They include the nonthermal sources Crab Nebula, IC 443, and 13S6A. Another source is 30 Doradus, which is the very large HII nebula or group of nebulae in the Large Cloud of Magellan. Three sources have a comparatively weak continuum temperature: 1404−51, 4·5°K; 1442−59, 4·5°K; and source B (NGC 6334), 11°K. Source 1441−59 has a possible line at −36 km/sec. No line was observed in Sagittarius A. Preliminary observations of Sagittarius B2 gave indications of the 126α line at +74 km/sec, but two later series over different velocity ranges near this value gave a negative result. A similar effect was found with a feature indicated at −113 km/sec in source 1618−49 by the preliminary observations.

(iv) *Very Broad Profiles*

In some cases the observed profile widths were so broad that it was obvious that more than one component must be present. Broad profiles have been divided into separate line contributions in a somewhat arbitrary fashion using such indications as changes in the envelope shape and suggestions of peaks. The halfwidths of these lines are given in parentheses in Table 1. The sources were η Carinae II, 1308−62 I, 1308−62 II, 1549−54, 1617−50 II, and 1618−49.

(v) *Average Values from Table 1*

Average values may be calculated from 55 entries in Table 1 for the following quantities

$$(T_l/T_c)_{av} = 3\cdot4\% \pm 1\cdot3\% \text{ s.d.} \quad (\text{Max. } 7\cdot1\%, \text{ min. } 1\cdot2\%);$$

$$(\Delta\nu)_{av} = 340 \text{ kHz} = 31\cdot5 \text{ km/sec};$$

$$\{(T_l/T_c)\Delta\nu\}_{av} = 1\cdot1 \times 10^4 \text{ Hz}.$$

TABLE 2

COMPARISON OF RADIAL VELOCITIES AND HALFWIDTHS AT OTHER LINES

All values are in units of km/sec

Source	109α R.V.	Δν	104α R.V.	Δν	158α R.V.	Δν	166α R.V.	Δν	126,127α R.V.	Δν
Orion Nebula	−2·0	29·0	−2	39·1	−4·9	37·1	0	45·2	−7*	38
Orion Δα−3′	−9·5	47·7							−7*	32
Orion Δα+3′	−2·4	28·6							−5*	31
Orion Δδ−3′	−7·0	36·3							−7*	38
Orion Δδ+3′	−2·6	27·5							+1*	38
NGC 2024	+4·4	22·4			+5·9	26·7			+4	21
RCW 38							+8	32·8	+1	30
NGC 6334					−5·1	25·8			−4	35
NGC 6357I	−1·2	26·9							−5	34
NGC 6357III	−5·9	31·5			−3·2	31·2			−1	34
M 8	+3·5	24·1			+4·6	24·2			−4	32
M 17 } Omega Nebula }	+17·6	38·5	+28	37·5	+18·3 / +25 } / +21 }	41·8 / 42·3	+20 / +20	42·7 / 38·5	+10 } / +19 } +17* / +32 }	36
M 17 Δα−4′	+16·3	35·2							+18*	32
M 17 Δα+4′	+17·5	32·6							+16*	36
M 17 Δδ−4′	+16·8	30·3							+19*	34
M 17 Δδ+4′	+13·3	38·6							+16*	36
W 43	+88·6	41·7	+93	28·7	+97·0	32·1			+89	27
W 49	+7·4	26·6	+17	31·3	+5·2	32·4			+7	26
W 51	+40·9	41·5	+53	28·7	+57·6	25·0			+55	37
Mean Δν		32·8		33·1		30·6				32·5

* Median values.

V. DISCUSSION OF RESULTS

(a) *Comparison with Other Results*

A comparison of the values of radial velocities and halfwidths from five excited Hα lines over 19 positions is made in Table 2. The 109α line was observed by Mezger and Höglund (1967), the 104α by Gudnov and Sorochenko (1966), the 158α by Lilley *et al.* (1966) and Dieter (1967), and the 166α by Palmer and Zuckerman (1966) and McGee and Gardner (1967). In many cases the agreement in radial velocity is satisfactory but in M 8, W 49, and W 51 differences of 10 km/sec and more are noted.

The halfwidths, usually stated in kilohertz by the above authors, have been converted to kilometres per second. The mean halfwidths of the values in Table 2 for four of the lines are within 1 km/sec of 32·5 km/sec; large individual differences occur in some sources.

In considering values of T_1/T_c from the five α-lines, mean spectra of T_1/T_c with ν have been plotted in Figure 2 for 11 sources. Additional data were available for the Orion and Omega nebulae (Meeks, personal communication). Mean values of all measurements for four lines are shown as circles. The 109α mean value appears higher than would be expected from the trend of the others. Some of the spread could well be caused by different estimates of the relevant thermal continuum temperature.
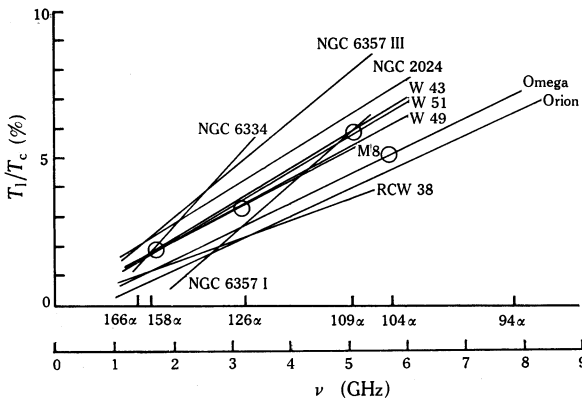
Fig. 2.—Line-to-continuum intensity ratio T_1/T_c as a function of frequency ν for 11 sources for lines between 94α and 166α. Mean values ($\bigcirc$) were available at 158α, 126α, 109α, and 104α.

(b) Location of HII Regions using the Excited H-line Radial Velocities

The location of HII regions, on the assumption that the radial velocities of the nebulae and the excited H lines must be reasonably close, could be attempted in the same way as was outlined for OH clouds by McGee, Gardner, and Robinson (1967). Dieter (1967) and Mezger and Höglund (1967) have positioned about 30 of the northern sources by similar means. In the present survey the majority of the sources lie in the area of positional ambiguity and have no optical identifications. Thus we have decided not to attempt locations until more comprehensive data become available.

(c) Comparison of Radial Velocities of Excited Hydrogen and Other Interstellar Constituents

The interstellar constituents of interest in this comparison are the ionized gases of the nebulae and the neutral gases in their immediate vicinity. Unfortunately, optical radial velocities of ionized gas could be found for only 5 of the present sources. Hydroxyl radial velocities may be compared in 11, HI absorption in 9, and HI emission velocities have been listed for each of the 11. The comparisons are made in Table 3. Some agreements may be seen but the data are too scanty for useful conclusions.

TABLE 3

COMPARISON OF RADIAL VELOCITIES OF IONIZED AND NEUTRAL GASES

Nebula	Radial Velocity (km/sec) of:				
	Excited H	Ionized H*	OH Gas*	HI Absorption*	HI Emission*
Orion Nebula	−10, +1, +18 } −7 med.	−6 to +8[a]†	+8, +3, +21	+4·5, +2·5[d]	+8[e]
NGC 2024	+4	+13·3[b]	+10		+6[e]
RCW 38	+1		+1, +3	+3·8, −4·2[d]	+3, +58[e]
η Carinae I+II	−20, −40, −1	−22·9[b], −36·6[a]	−21	−12	−15, +18, +36[e]
NGC 6334	−4		−5, +6	−5·7, +4·2[d]	−6[e]
NGC 6357II	−1		−11, −6, +1, +5	−12·7, −1·3, +4·9, +11·4[d]	−6[e]
M 8	−4 (+4)	+7·5[b], +8·7[a]	+10[c]	0, +6·3[d]	−8, +6[e]
M 17	+10, +19, +32 } +17 med.	+25·1[b], +21[a]	+20	+6·9, +14·5, +20·7, +6·3[d], +26·4	−21, +21[e]
W 43	+89		+7·5, +12·5, +81·5, +89·5[c], +94	+12·7, +54·9, +83·6[d]	+18, +43, +97[e]
W 49	+7		+6, +13, +16, +18, +22		+12[e]
W 51	+55		+5·8, +51, +64[c]	+7·2, +12·7, +47·5, +54·9[d]	+12[e]

* References are: a, Wilson *et al.* (1959); b, Courtès, Cruvellier, and Georgelin (1967); c, Goss (1967); d, Clark (1965); e, McGee, Milton, and Wolfe (1966).

† For the lines [OIII], [OII], and Hγ.

Ionized gas. A further difficulty is that, whereas the excited hydrogen observations are centred on the positions of the radio continuum maxima and probably represent an average because of beamwidth limitations, the Hα velocities quoted in the table (Courtès, Cruvellier, and Georgelin 1967) have been measured in filaments of much smaller size comparatively and in general not in the central positions. Dieter (1967) found a velocity correlation in 6 of 12 cases.

Hydroxyl gas. Table 1 contains 22 cases of corresponding radial velocity measurements of the excited hydrogen and hydroxyl gas. In 9 cases values agreed within 2 km/sec. Differences between nearest values for all range between ±18 km/sec (with one −37 km/sec). However, the sources of recombination H lines are intrinsically associated with HII regions but hydroxyl gas has been shown to exist frequently in neutral hydrogen regions away from the nebulae.

Neutral hydrogen absorption. At least one radial velocity value in each of the nine sets in Table 3 indicates that an HI cloud must lie in front of and fairly close to a corresponding HII region.

Neutral hydrogen emission. The HI emission velocities are taken from peaks of profiles observed in the directions of the 11 sources in Table 3. One of the values in each set is typical of the HI gas cloud surrounding the particular nebula.

(d) *Excited H-line Halfwidths*

We now discuss what is perhaps the most important result of this investigation. In all the published reports to date authors have been content to fit Gaussian curves to rather noisy sets of intensity readings spread across the expected frequency band. The halfwidth of the single Gaussian shape, corrected for instrumental bandwidth, has been used to calculate the kinetic temperature of the electrons in the HII nebulae in formulae similar to equation (3).

If the values for T_1/T_c of $0 \cdot 034$ and $\Delta\nu$ of 340 kHz stated in Section IV (a) (v) are substituted in equation (3), a mean kinetic temperature of $5\,500°$K may be read from Figure 1 for $n = 126$, $u = 0 \cdot 15$ (line A) under conditions of local thermodynamic equilibrium $(b_n = 1)$. This is in excellent agreement with the values of $5\,800°$K found by Mezger and Höglund (1967) from 109α measurements and $5\,200°$K by Dieter (1967) from 158α results.

On the other hand, optical determinations for T_e in HII nebulae have given a value of about $10\,000°$K. Pottasch (1965) has shown that the average value over a number of nebulae may be lower and that T_e varies in the nebula itself, but no value comes as low as $5\,800°$K.

Recently Peimbert (1967), using intensity ratios of auroral to nebular forbidden lines and of bound–free continuum to bound–bound emission lines of hydrogen for some HII regions, concluded that temperature fluctuations inside nebulae have a significant effect on values of electron temperatures determined from different physical processes. For example, temperatures derived from the Balmer jump and forbidden lines showed fluctuations of a few thousands of degrees ($10\,500$–$13\,700°$K) in the Orion Nebula.

A certain amount of controversy has appeared in recent literature with attempts to explain the differences in optical and radio results. Goldberg (1966) has pointed out that a departure from local thermodynamic equilibrium may be the cause (see Fig. 1) and that db_n/dn (Seaton 1964) is important in gaseous nebulae The present authors (Gardner and McGee 1967) have offered some experimental results supporting Goldberg's arguments.

It should be kept in mind that, if the profile departs from the Gaussian shape, $T_1\Delta\nu$ must be replaced by $\int T_1\,d\nu$. The estimation of T_e depends on the area under the curve. The estimation of turbulence velocities depends on the halfwidths.

In general the sensitivity level leaves much to be desired and most of the sources have been observed for the minimum possible time that is consistent with producing the line "signal". However, the two most important sources Orion and Omega nebulae have received much more attention. In the first series of 126α observations in September 1966 it was noticed that the two profiles were not simple single-peaked curves. For Orion, peaks in the profile were discernible near −10, +1, and +18 km/sec and for Omega, peaks at +9, +19, and +32 km/sec. In earlier notes (McGee and Gardner 1967) we have quoted median radial velocity values (there was a possibility that the peaks were caused by instrumental effects). However, with further 126α and 127α line observations in March 1967 the three profile peaks were again recorded in each case. It will be remembered that the receiver conditions were completely different for the 127α line (Section III).

(i) *Orion Nebula*

In showing how the complex profile for the Great Nebula in Orion fits in with current ideas, the surrounding envelope and the radio and optical evidence for the motions in and near the nebula are briefly discussed.

One of us (R. X. McG.) has made a survey of neutral hydrogen in the region of ∼ 45′ radius from θ^1 Ori using a 14′·5 aerial beam. The HI intensity contours reveal the striking absorption dip ($T_a \sim$ −150 degK) coincident with the visible ionization region. Although the earlier low resolution observations did not indicate any significant change in the line emission in the vicinity, the present beam was able to distinguish a fairly well-defined cloud of HI surrounding the nebula. The velocity information substantiates this. The "expected" emission HI profile at the continuum maximum is given in Figure 3 (curve C). The peak radial velocity is +8 km/sec, which is approximately the kinematical model velocity at the distance of Orion. The asymmetry in the negative wing is repeated in all the surrounding emission profiles. It corresponds closely in velocity to the absorption indicated in Figure 3 by the halfwidth spacing −5 to +6 km/sec and the maximum absorption velocity +2·5 km/sec. Thus we can distinguish HI gas in front of and behind the nebula and in both cases it is probable that such gas is in its immediate neighbourhood. The halfwidth of the positive component +2·5 to +13·5 km/sec has the same value, 11 km/sec, as the absorption line profile.

The OH line observations in the direction of the Orion Nebula have been discussed by McGee, Gardner, and Robinson (1967). The results were unusual in that a very broad emission line profile was recorded at 1665 MHz over the total velocity

range −16 to +36 km/sec—the same overall width as the HI profile. Narrow-band peaks similar to those at other HII regions were superimposed at +3, +7, and +21 km/sec. Goss (1967) has published profiles at the four OH lines, from which we note almost the same features at 1665 MHz after allowing for his improved frequency resolution. Absorption features at +6 and +8 km/sec are seen in the 1667 and 1720 MHz lines. We do not attempt to explain the wide-band emission, but we do know from other observations (McGee, Gardner, and Robinson 1967) that the narrow-band emission comes from areas at the edges of HII regions and that the absorbing hydroxyl gas may be spread through the HI cloud.
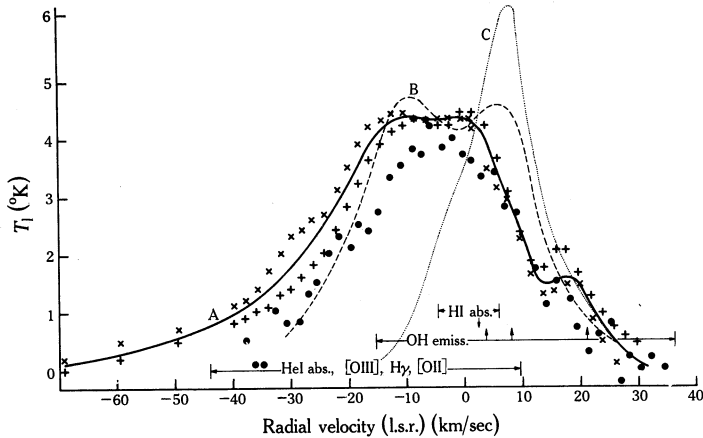
Fig. 3.—Line profiles for the Orion Nebula: curve A, composite recombination line from 126α (+) and 127α (×) measurements; ●, points from the 158α profile; curve B, double [OIII] line profile; curve C, expected HI profile. The HI line absorption is shown as a halfwidth range and the OH line emission as an overall range. The velocities at intensity maxima are marked. The velocity range of optical lines is taken from Wilson *et al.* (1959). The T_1 scale applies only to 126α and 127α lines.

The neutral hydrogen and hydroxyl gas then form the outer envelope of the nebula. The hydrogen gas in which the recombination lines form has always been found in the direction of maximum continuum emission. The composite 126α–127α line profile is given in Figure 3 (curve A). Dieter's (1967) observation points for 158α, suitably scaled, are superimposed. Peaks can be seen near −10, +1, and +18 km/sec radial velocity. The halfwidth extends from −26 to +11 km/sec (37 km/sec). Therefore the profile contains a component or components that are more negative in radial velocity than the HI and OH. It may be inferred that a large proportion of the excited hydrogen is expanding outwards in our direction. In the opposite direction expansion is not so obvious, except for the presence of the moderately intense component at +18 km/sec.

It should be noted that we are pointing to three main peaks in the profile as evidence of a number of large-scale motions. If the broadening was caused by turbulence then the observed profile would be truly Gaussian in shape.

However, Goss (personal communication) has pointed out that the observation of different radial velocities across the nebula by Mezger and Höglund (1967) and the

present authors (see Section IV (*a*) (i)) clearly indicates that two or more large-scale motions are present and hence doubts must be cast on the derivation of large values of turbulent velocities (+17 km/sec by Mezger and Höglund, and +32 km/sec by Dieter for the Orion Nebula) from the single Gaussian. Two recent investigations seem to establish this view beyond doubt. Mills and Shaver (1967) have resolved the main body of the Orion Nebula, NGC 1976, and its northerly companion NGC 1982 as separate radio sources 7'·5 arc apart. Gordon and Meeks (1968) using the H 94α line report a radial velocity of −3 km/sec for NGC 1976 and +7 km/sec for NGC 1982.

The velocity range of the recombination line profile is paralleled by the radial velocities of the optical lines. Wilson *et al.* (1959) measured velocities at several thousand points over an area 4' by 4' centred on the Trapeziuun (θ^1 Ori). They found that the overall mean radial velocity of OIII is about −10 km/sec with respect to the Trapeziuun stars, which was interpreted as an expansion of the HII region into the surrounding cold gas. Different velocities for constituents [OIII], Hα, [OII] were found to be caused by the different ionization potentials. Absorption lines for HeI were also measured. The typical halfwidth for an Hγ line was measured as 29 km/sec. In many places the lines became considerably broader and even distinctly double with separations up to 25 km/sec. A double [OIII] line (curve B) has been included in Figure 3 from details given in Figure 7 of Wilson *et al.* (1959). Its halfwidth is almost identical with the recombination profile. The approximate range of the optical velocities is also marked in Figure 3.

Weedman (1966) has shown that if these optical data are considered as distributed over the area of the aerial beam (6'·4 arc) of Höglund and Mezger (1965) and are subject only to optical instrumental broadening effects a Gaussian profile similar to the radio case will result. The width measured by Höglund and Mezger was 29 km/sec, but other observers report widths near 38 km/sec for the Orion Nebula (Table 2).*

(ii) *Omega Nebula*

The recombination H line profile at 126α for the Omega Nebula (M 17) is shown in Figure 4. Again we have taken the 10 kHz points from the 158α profile (Dieter 1967) and scaled them to fit on our diagram. The agreement is good. The presence of at least two major components of motion is strongly supported by the observations of Zisk (1966) in the λ2 cm continuum. With a 2'·3 arc aerial beam M 17 is resolved into two distinct sources 3'·5 arc apart. Dieter (1967) refers to these in commenting on the large halfwidth of the 158α line. In the present work the 6' beam centred on the apparent maximum at 3249 MHz intercepted major contributions from both sources. The change of 3 km/sec in the median radial velocities in the north-east and south-west of the nebula (Section IV (a) (i)) may be further evidence of components of differing velocities.

* *Note added in proof.* We are indebted to Dr. P. Palmer of the Harvard College Observatory for comments on Figure 3. He finds that, except for the flat top and the +18 km/sec feature, fair agreement with recent observations of the 94α line (Gordon and Meeks 1968) and the 109α line (Palmer, personal communication) is possible if a baseline of slope −1/110 degK km^{-1} sec^{-1} is assumed for curve A in Figure 3.

The observed profile was approximated fairly well by three computer-produced Gaussian curves with the following parameters:

Radial velocity (km/sec)	$+2 \cdot 7$	$+18 \cdot 4$	$+34 \cdot 5$
Maximum T_1 (°K)	$2 \cdot 7$	$5 \cdot 0$	$1 \cdot 8$
Halfwidth (km/sec)	$18 \cdot 5$	$20 \cdot 9$	$17 \cdot 5$

These values do not constitute a unique solution but they indicate the halfwidths that may be expected and how great the error in turbulence may be if a single Gaussian curve represents this profile.
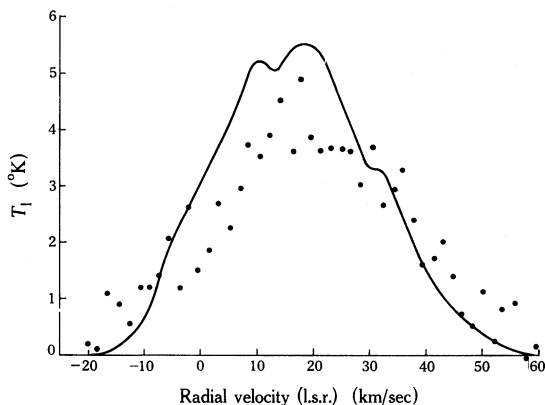
Fig. 4.—Line profiles for the Omega Nebula. The curve is the recombination line for 126α while the points are from the 158α profile. The T_1 scale applies only to the 126α line.

(iii) *Other Nebulae*

Wide profiles that were not quite resolved into separate components were observed in several sources. They are not the "very broad" cases mentioned in Section IV (*a*) (iv). The signal-to-noise ratio was much lower than for (i) and (ii) above so that, in general, median values of radial velocity had to be given in Table 1. Some notes on these sources follow.

RCW 38. The nebula consists of four concentrations of Hα in an area 40′ by 40′. Thus it is reasonable to expect differing velocity components.

RCW 36. Three bright S-shaped Hα regions in an area 12′ by 6′ imply differing motions.

η Carinae. The two continuum maxima of sources I and II are about 8′ arc apart at 3 249 MHz. The complex profile is in source I. The two components of source II given in Table 1 are clearly separate in the observed profile.

1109—61 and RCW 57. These are neighbouring sources.

NGC 6334. The Table 1 entry for the radial velocity is −4 km/sec but there is evidence of a secondary peak near +6 km/sec.

NGC 6357 II. The value in Table 1 of −1 km/sec is median. Components possibly exist at −6 and +4 km/sec.

We sum up this section by suggesting that the primary cause of the wider recombination H line profiles is the presence of two or more components representing differing radial velocities of filaments or other large-scale concentrations in motion

in the HII regions. However, the problem is not yet solved. The recognition of such components has been achieved with the aid of frequency resolution in the line observations. The corresponding values of the continuum thermal emission T_c of these components are not obtained at the present angular resolution.

Two conclusions result: (1) the electron temperature T_e for any particular filament is unlikely to exceed the optically derived values ($\sim 10^4\,°K$), and (2) the electron temperatures for all individual filaments or clouds are likely to be higher than the values derived by simply taking $(T_l/T_c)\Delta\nu$ for the whole line profile. In addition, the possibility of departures from low opacity in the continuum and from local thermodynamic equilibrium requires consideration.

VI. CONCLUSIONS

The survey of 40 sources for the presence of radiation from excited hydrogen in the two lines 126α and 127α near 3200 MHz has provided a useful "midpoint" in the overall preliminary investigation of this aspect of the interstellar medium.

Evidence has been presented to show that, as far as present equipment sensitivities will allow, the excited hydrogen occurs in association with all HII nebulae or thermal emitters. Thus with the improved receivers already coming into use and increased angular resolution much data will become available to greatly enhance the study of galactic structure.

The necessity for caution in making calculations of electron temperature and turbulence in HII regions from the observed quantities T_l/T_c and $\Delta\nu$ has been shown. In some outstanding cases the observed recombination line profiles are not, in fact, of a simple Gaussian shape but exhibit two or more peaks. Improved angular resolution, even to 2' or 3' arc, would contribute much towards accurate estimates of the properties of HII regions.

VII. ACKNOWLEDGMENTS

VIII. REFERENCES

CLARK, B. G. (1965).—*Astrophys. J.* **142**, 1398–422.
COHEN, E. R., and DU MOND, J. W. M. (1965).—*Rev. mod. Phys.* **37**, 537–94.
COURTÈS, G., CRUVELLIER, P., and GEORGELIN, Y. (1967).—*Publs Obs. Hte Provence* **8**, 34.
DIETER, NANNIELOU H. (1967).—*Astrophys. J.* **150**, 435–51.
DRAVSKIKH, Z. V., and DRAVSKIKH, A. F. (1964).—*Astr. Tsirk. Byuro astr. Soobshch.* No. 292.
GARDNER, F. F., and McGEE, R. X. (1967).—*Nature, Lond.* **213**, 480–1.
GOLDBERG, L. (1966).—*Astrophys. J.* **144**, 1225–9.

GORDON, M. A., and MEEKS, M. L. (1968).—Observations of 8 GHz continuum and hydrogen recombination lines in the Orion Nebula. *Astrophys. J.* (in press).

GOSS, W. M. (1967).—OH absorption in the Galaxy. *Astrophys. J. Suppl. Ser.* 15, No. 137 (in press).

GUDNOV, V. M., and SOROCHENKO, R. L. (1966).—Emission of excited hydrogen line $n_{105}-n_{104}$ in certain nebulae in the Northern Sky. Fizicheskii inst. imeni P.N. Lebedev Akad. nauk S.S.S.R. Lab. Rad. Astr. Moskva.

HÖGLUND, B., and MEZGER, P. G. (1965).—*Science, N.Y.* 150, 339–48.

KARDASHEV, N. S. (1959).—*Astr. Zh.* 36, 838–44. Translated (1960) in *Soviet Astr.* 3, 813–19.

LILLEY, A. E., MENZEL, D. H., PENFIELD, H., and ZUCKERMAN, B. (1966).—*Nature, Lond.* 209, 468–70.

McGEE, R. X., and GARDNER, F. F. (1967).—*Nature, Lond.* 213, 579.

McGEE, R. X., GARDNER, F. F., and ROBINSON, B. J. (1967).—*Aust. J. Phys.* 20, 407–20.

McGEE, R. X., MILTON, JANICE A., and WOLFE, WENDY (1966).—*Aust. J. Phys. Astrophys. Suppl.* No. 1.

McGEE, R. X., and MURRAY, J. D. (1963).—*Proc. Instn Radio Engrs Aust.* 24, 191–6.

MENZEL, D. H. (1937).—*Astrophys. J.* 85, 330–9.

MENZEL, D. H., and PEKERIS, C. L. (1935).—*Mon. Not. R. astr. Soc.* 96, 77–111.

MEZGER, P. G., and HÖGLUND, B. (1967).—*Astrophys. J.* 147, 490–518.

MILLS, B. Y., and SHAVER, P. (1967).—Cornell–Sydney University Astr. Centre Preprint No. 69.

OSTER, L. (1961).—*Rev. mod. Phys.* 33, 525–43.

PALMER, P., and ZUCKERMAN, B. (1966).—*Nature, Lond.* 209, 1118.

PEIMBERT, M. (1967).—*Astrophys. J.* 150, 825–34.

PENFIELD, H., PALMER, P., and ZUCKERMAN, B. (1967).—*Astrophys. J.* 148, L25–8.

POTTASCH, S. (1965).—*Vistas Astr.* 6, 149–206.

SEATON, M. J. (1964).—*Mon. Not. R. astr. Soc.* 127, 177–84.

SOROCHENKO, R. L. (1965).—Akad. nauk S.S.S.R. Fizicheskii inst. Trudy 28, 65–72. Translated by Consultants Bureau, New York (1966).

SOROCHENKO, R. L., and BORODZICH, E. V. (1964).—Paper presented at 12th Gen. Ass. IAU, Hamburg (unpublished).

WEEDMAN, D. W. (1966).—*Astrophys. J.* 145, 965–7.

WILD, J. P. (1952).—*Astrophys. J.* 115, 206–21.

WILSON, O. C., MÜNCH, G., FLATHER, EDITH M., and COFFEEN, MARY F. (1959).—*Astrophys. J. Suppl. Ser.* 4(40), 199–256.

ZISK, S. H. (1966).—*Science, N.Y.* 153, 1107–9.